

# Aggregation and Self-Assembly of Amphiphilic Block Copolymers in Aqueous Dispersions of Carbon Nanotubes

Rina Shvartzman-Cohen,<sup>†</sup> Marc Florent,<sup>‡,§</sup> Daniella Goldfarb,<sup>§</sup> Igal Szleifer,<sup>||</sup> and Rachel Yerushalmi-Rozen<sup>\*,†,‡</sup>

Department of Chemical Engineering and the Ilse Katz Institute for Nanoscale Science and Technology, Ben-Gurion University of the Negev, 84105 Beer Sheva, Israel, Department of Chemical Physics, the Weizmann Institute of Science, 76100 Rehovot, Israel, and Department of Biomedical Engineering, Northwestern University, 2145 Sheridan Road, Evanston, Illinois 60208

Received December 3, 2007. In Final Form: January 10, 2008

The self-assembly (SA) of amphiphilic block copolymers (poly(ethylene oxide)–poly(propylene oxide)–poly(ethylene oxide)) was investigated in dispersions of single-walled and multiwalled carbon nanotubes (SWNT and MWNT, respectively) as a function of temperature. Differential scanning calorimetry (DSC) was used for characterization of the thermal behavior of the combined polymers–nanostructures system, and spin-probe electron paramagnetic resonance (EPR) was employed for probing the local dynamic and polarity of the polymer chains in the presence of nanostructures. It was found that SWNT and MWNT modify the temperature, enthalpy, and dynamic behavior of polymer SA. In particular, SWNT were found to increase the cooperativity of aggregating chains and dominate aggregate dynamics. MWNT reduced the cooperativity, while colloidal carbon black additives, studied for comparison, did not show similar effects. The experimental observations are consistent with the suggestion that dimensional matching between the characteristic radius of the solvated polymer chains and the dimensions of additives dominate polymer SA in the hybrid system.

## Introduction

Over the past few years, block copolymers<sup>1</sup> have been utilized for modifying the solution behavior of nanostructures including nanoparticles,<sup>2–4</sup> nanorods,<sup>5</sup> and carbon nanotubes (CNT).<sup>6,7</sup> Block copolymers were shown to disperse nanostructures and colloidal moieties<sup>8,9</sup> in different media and to induce their assembly into mesostructures.<sup>10–12</sup> Recently, it was suggested that block copolymers may be used as a vehicle for directing functional nanostructures (nanoparticles, nanotubes) onto surfaces.<sup>13</sup> An important prerequisite for utilization of block copolymers for shaping the assembly of nanostructures is the development of an understanding of the interactions that dominate the behavior of the combined systems. Nanostructures may affect the phase behavior, dynamics, and mechanisms of self-association in polymers–nanostructures–solvent systems. Detailed char-

acterization of those systems, from the molecular to the macroscopic level, provides a difficult challenge both for experiment and theory.

Among the most useful block copolymers are the amphiphilic block copolymers poly(ethylene oxide)–poly(propylene oxide)–poly(ethylene oxide), PEO<sub>y</sub>PPO<sub>x</sub>PEO<sub>y</sub> (Poloxamers (ICI) or Pluronics (BASF)). Pluronic block copolymers are known to self-assemble in water into micelles consisting of a hydrophobic core of PPO and a corona of the solvated PEO. It is accepted that the driving force for micellization in aqueous solutions is entropic.<sup>14</sup> Micellization is initiated (at a fixed temperature) by increasing the concentration to above the critical micellar concentration, CMC, or by increasing the temperature (at a given concentration) to above the critical micellization temperature, CMT.<sup>15,16</sup> An important observation is that the CMC and CMT are highly sensitive to the presence of molecular additives,<sup>17–21</sup> while colloidal particles, such as carbon black (CB), do not affect polymer self-assembly (SA) and do not alter the structure of the formed micelles.<sup>8</sup> What should one expect when nanostructures, such as carbon nanotubes (CNT), are present in solutions of self-assembled polymers?

\* To whom correspondence should be addressed. Telephone: 972-8-6461272. Fax: 972-8-6472916. E-mail: rachely@bgu.ac.il.

<sup>†</sup> Department of Chemical Engineering, Ben-Gurion University.

<sup>‡</sup> The Ilse Katz Institute for Nanoscale Science and Technology, Ben-Gurion University.

<sup>§</sup> The Weizmann Institute of Science.

<sup>||</sup> Northwestern University.

(1) Ruzette, A. V.; Leibler, L. *Nat. Mater.* **2005**, *4*, 19–31.

(2) Qi, L.; Cölfen, H.; Antonietti, M. *Nano Lett.* **2001**, *1*, 61–65.

(3) Sakai, T.; Alexandridis, P. *Langmuir* **2004**, *20*, 8426–8430.

(4) Tadd, E.; Zeno, A.; Zubris, M.; Dan, N.; Tannenbaum, R. *Macromolecules* **2003**, *36*, 6497–6502.

(5) Zhang, Q.; Gupta, S.; Emrick, T.; Russell, T. P. *J. Am. Chem. Soc.* **2006**, *128*, 3898–3899.

(6) Shin, H.-I.; Min, G. B.; Jeong, W.; Park, C. *Macromol. Rapid Commun.* **2005**, *26*, 1451–1457.

(7) Szleifer, I.; Yerushalmi-Rozen, R. *Polymer* **2005**, *46*, 7803.

(8) Lin, Y.; Alexandridis, P. *J. Phys. Chem. B* **2002**, *106*, 10834–10844.

(9) Napper, D. H., Ed. *Polymeric Stabilization of Colloidal Dispersions*; Academic Press, Inc.: Orlando, FL, 1993.

(10) Lin, Y.; Böker, A.; He, J.; Sill, K.; Xiang, H.; Abetz, C.; Li, X.; Wang, J.; Todd, E.; Long, S.; Wang, Q.; Balazs, A.; Russell, T. P. *Nature* **2005**, *434*, 55–59.

(11) Cölfen, H.; Mann, S. *Angew. Chem., Int. Ed.* **2003**, *42*, 2350–2365.

(12) Lazzari, M.; López-Quintela, M. A. *Adv. Mater.* **2003**, *15*, 1583–1594.

(13) Nap, R.; Szleifer, I. *Langmuir* **2005**, *21*, 12072–12075

(14) Maibaum, L.; Dinner, A. R.; Chandler, D. *J. Phys. Chem. B* **2004**, *108*, 6778–6781.

(15) Wanka, G.; Hoffman, H.; Ulbricht, W. *Macromolecules* **1994**, *27*, 4145–4159.

(16) *Amphiphilic Block Copolymers: Self-Assembly and Applications*; Alexandridis, P., Lindman, B., Eds.; Elsevier: Amsterdam, Lausanne, New York, Oxford, 2000.

(17) Steinbeck, C. A.; Hedin, N.; Chemelka, B. F. *Langmuir* **2004**, *20*, 10399–10412.

(18) Electrolytes are known to lower the CMT; see, for example, Jain, N. J.; Aswal, V. K.; Goyal, P. S.; Bahadur, P. *J. Phys. Chem. B* **1998**, *102*, 8452–8458.

(19) The effect of molecular additives is general and spans beyond purely aqueous media; see, for example, Zhang, L.; Yu, K.; Eisenberg, A. *Science* **1996**, *272*, 1777–1779.

(20) Nonelectrolytes may either lower or raise the CMT. Armstrong, J. K.; Chowdhry, B. Z.; Mitchell, J.; Beezer, A.; Leharne, S. *J. Phys. Chem.* **1996**, *100*, 1738–1745 and ref 21.

(21) Alexandridis, P.; Athanassiou, V.; Hatton, T. A. *Langmuir* **1995**, *11*, 2442–2450.

**Table 1. Composition of PEO–PPO–PEO Copolymers**

polymer	MW	no. of EO units	no. of PO units	PEO wt %	product no.
P84	4200	34	39	40%	586440
F88	11 400	200	40	80%	560840
P103	4950	32	56	30%	586460
P104	5900	50	56	40%	589640
F108	14 600	260	60	80%	583062
P123	5750	40	70	30%	587440
F127	12 600	212	70	70%	583106

CNT are cylindrical structures with a typical diameter of 0.8–2 nm for single-walled nanotubes (SWNT) and 10–40 nm for multiwalled nanotubes (MWNT) and a length of up to millimeters, resulting in a large aspect ratio of >1000 and a relatively large surface area.<sup>22</sup> The graphitic CNT are hydrophobic and characterized by a large and non-isotropic polarizability.<sup>22</sup> Unlike classical colloids that are dominated by long-ranged dispersive forces, nanometric objects such as CNT (and fullerenes) interact via short-ranged intermolecular potential.<sup>23,24</sup>

In this study, we investigate temperature induced SA in the combined carbon nanotubes–Pluronics–water system. Differential scanning calorimetry (DSC) is used to characterize the micellization temperature and enthalpy in dispersions of SWNT and MWNT. The macroscopic characterization is complemented by molecular information obtained via spin-probe electron paramagnetic resonance (EPR), reported in detail in ref 25. The latter enables the investigation of the local polarity and motional characteristics of the polymers and probes the transition from individual chains to micelles. Based on the results obtained by the two methods, we suggest a mechanism for self-aggregation of Pluronics in the presence of nanostructures.

### Experimental Section

**Materials.** *Polymers.* Different water soluble Pluronics triblock copolymers were received as a gift from BASF AG Germany and used as received (Table 1).

*Carbonaceous Materials.* Raw SWNT synthesized by arc discharge were purchased from two different sources and used as received: (1) NanoCarbLab (NCL) Russia ([www.nanocarblab.com](http://www.nanocarblab.com)); according to the specifications by the manufacturer, the as-prepared grade consists of 80 vol % SWNT and impurities of graphite and the metal catalyst. (2) Carbolex Inc. (SWNT (AP) <http://carbolex.com>); according to the specifications by the manufacturer, the as-prepared AP grade consists of 50–70 vol % SWNT and impurities include approximately 35 wt % graphite cobalt and nickel.

MWNT produced by catalytic chemical vapor deposition were purchased from INP, Toulouse, France. The powder contains 95 vol % MWNT, and the tube diameters are above 20 nm with lengths of micrometers and specific areas of 700–1000 m<sup>2</sup>/g.

A dry powder of carbon black (CB), Vulcan P grade, was purchased from Cabot Corp. and used as received. Typical values of specific area are 700–1000 m<sup>2</sup>/g, and typical diameters of the primary particles are 30–50 nm.

**Sample Preparation.** Aqueous solutions of the block copolymers were prepared by dissolving a block copolymer in water at room temperature to form solutions of desired concentrations. The solutions were mixed for about 2–3 days using a magnetic stirrer or a roller. Required spin probes were then added to the final concentration (in the range of 0.1–0.5 mM).

(22) Dresselhaus, M. S.; Dresselhaus, G.; Avouris, Ph., Eds. *Carbon Nanotubes*; Topics in Applied Physics Series 80; Springer-Verlag: Berlin, Heidelberg, 2001.

(23) Girifalco, L. A.; Hodak, M.; Lee, R. S. *Phys. Rev. B* **2000**, *62*, 13104–13110.

(24) Shvartzman-Cohen, R.; Nativ-Roth, E.; Baskaran, E.; Levi-Kalishman, Y.; Szeleifer, I.; Yerushalmi-Rozen, R. *J. Am. Chem. Soc.* **2004**, *126*, 14850–14857.

(25) Florent, M.; Shvartzman-Cohen, R.; Goldfarb, D.; Yerushalmi-Rozen, R. *Langmuir*, **2008**, *24*, 3773–3779.

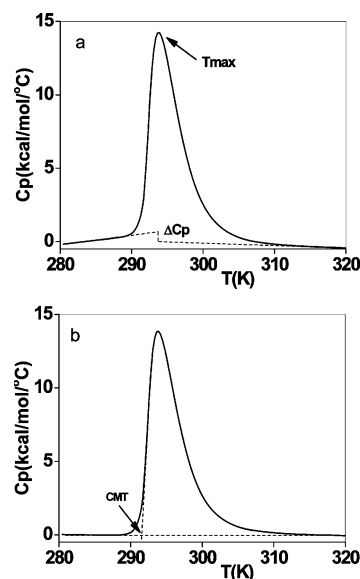


**Figure 1.** Normalized DSC trace (aqueous solution of 10 wt % F127) (a) before baseline fitting and (b) after baseline fitting following ref 27.  $\Delta C_p$ ,  $T_{max}$ , and CMT are marked by arrows.

Liquid dispersions of CNT or CB were prepared by sonicating the powder of the raw material (typical concentration of 0.5–1.0 wt %) at very mild conditions (50 W, 43 kHz) for 30–40 min in the polymeric solution.<sup>24,26</sup> The dispersions were centrifuged (at 4500 rpm for 30 min), and the supernatant was decanted from above the precipitate. As was shown before,<sup>24</sup> the dispersion process is selective toward CNT, and the precipitate mainly contains colloidal moieties. As some of the CNT precipitate, the effective CNT concentration in the resulting supernatant is somewhat lower than the initial concentration. Throughout the text, we designate initial concentrations.

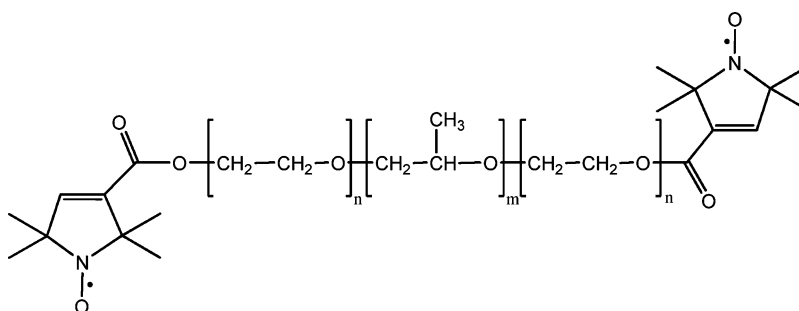
**Techniques and Methods.** *High Sensitivity Differential Scanning Calorimetry (HSDSC).* Microcal VP-DSC for HSDSC at a cell volume of 0.5 mL was used. The reported measurements were carried out at a scan rate of 1 K min<sup>-1</sup>, by heating from 280 to 360 K. The HSDSC instrument measures the power required to keep the temperature of the sample and reference cell equal while raising the temperature of the system at a constant rate. The output of the instrument is  $(dq/dt)_p$  vs  $t$ , where  $q$  is the heat and  $t$  is the time. The output is converted to the excess heat capacity ( $C_p$ ) vs temperature by multiplying the  $x$ -axis by the scan rate.<sup>27</sup> The baseline was fitted to the data using the Microcal software (Microcal Software Inc., Northampton, MA): This consisted of using the pre- and post-transitional data points to fit a spline curve. The calculated baseline data were subsequently subtracted from the HSDSC data. Exploratory measurements carried at different scan rates suggested that the calorimetric data was not affected by the scan rate. Heating and cooling sequences did not show hysteresis. To estimate the uncertainties in the measurement, multiple heating and cooling scans were carried out, suggesting an uncertainty of  $\pm 5\%$  in the calorimetric enthalpy and  $\pm 1^\circ$  in the measured values of CMT and  $T_{max}$ .

Figure 1 presents typical DSC thermograms of aqueous solutions of F127. The thermograms exhibit a broad and asymmetric endothermic peak. Four features may be used to characterize the transition (see Figure 1): (1)  $\Delta C_p$ , the negative change in the apparent heat capacity is associated with aggregation; (2)  $\Delta H_{cal}$ , the calorimetric enthalpy calculated from integration of the calorimetric trace of  $\Delta C_p$  measured vs temperature; (3)  $T_{max}$  the temperature at which  $C_p$  reaches a maximum, marking the maximal aggregation rate; and (4) the CMT is determined from the tangent at  $T_{onset} =$  CMT as indicated in Figure 1b, after baseline fitting. In addition,

(26) Nativ-Roth, E.; Shvartzman-Cohen, R.; Bounioux, C.; Florent, M.; Zhang, D.; Szeleifer, I.; Yerushalmi-Rozen, R. *Macromolecules* **2007**, *40*, 3676–3685.

(27) Armstrong, J.; Chowdhry, B.; O'Brien, R.; Beezer, A.; Mitchell, J.; Leharne, S. J. *Phys. Chem.* **1995**, *99*, 4590–4598.

Scheme 1



the steepness of the initial slope and the half-width of the peak provide qualitative measures of the aggregate size.<sup>28</sup>

Following Paterson et al.,<sup>28</sup> we note that the asymmetric calorimetric trace and the negative heat capacity change at the transition ( $\Delta C_p < 0$ ) are indicative of an aggregation process, such as micellization.  $\Delta H$  of the transition, as calculated from the peak area, is positive and results from the dehydration of PPO groups.<sup>29</sup>

**Spin-Probe EPR.** EPR spectra were recorded using an X-band Bruker Elexsys 500 spectrometer with a modulation amplitude of 0.3 G. The samples were placed in a flat quartz cell, and the temperature was controlled using the spectrometer temperature controller. For temperatures lower than room temperature, the sample was cooled by N<sub>2</sub> gas passing through an acetone/dry ice bath. The actual temperature was determined independently by a thermocouple located at the center of the cavity. Spectra were recorded while increasing and decreasing the temperature, with equilibration periods of 30 min between each step. Comparison of the heating and cooling sequences showed that the measurements are reversible and do not exhibit hysteresis.

**Spin Labeling.** Nitroxide spin labels are routinely used to obtain information by means of EPR in systems where no paramagnetic center is present. The EPR spectrum provides information on their motional characteristics in terms of rotational correlation times, their anisotropy, and order parameters, which reflect the properties of their environment.<sup>30</sup> Moreover, the polarity of a spin label's microenvironment can be probed by the isotropic <sup>14</sup>N hyperfine coupling,  $a_{\text{iso}}$ , which increases with increasing solvent polarity,<sup>31</sup> and therefore can be used to detect processes such as micellization.<sup>32,33</sup>

The nitroxide radicals are stable and only minute amounts are required such that their presence does not perturb the system. The properties of the nitroxide spin probe may be modified so as to target the label to different locations of the system under study. Due to these unique properties, nitroxide spin probes have been extensively used to probe structural and dynamic properties of micelles, liquid crystals, membranes, and proteins.<sup>30</sup> As micellization of Pluronics is associated with a change in polarity and mobility, a careful choice of spin probes can provide a reliable indication on different stages of the process.<sup>34,35</sup>

Here, we employed three nitroxide labeled Pluronics based on L62, P123, and F127, where a nitroxide spin label was placed at the end of each PEO chain. As the spin labels are attached to the terminal hydroxyl of the PEO chain, the EPR spectrum monitors the motion

of the PEO tails. The structure of L62-NO is schematically presented in Scheme 1. The spin probes were synthesized according to procedures described in the literature.<sup>36</sup>

**Electron Microscopy (EM).** Solutions of Pluronic block copolymers that contain dispersed SWNT and MWNT were characterized via direct imaging of the dispersions using cryo-transmission electron microscopy (cryo-TEM). Dried samples were imaged using high-resolution transmission electron microscopy (HRTEM).

Sample preparation for cryo-TEM measurements was carried out as follows: a drop of the solution was deposited on a TEM grid (300 mesh Cu grid) coated with a holey carbon film (lacey substrate, Ted Pella Ltd). The excess liquid was blotted, and the specimen was vitrified by rapid plunging into liquid ethane precooled with liquid nitrogen in a controlled environment vitrification system. The samples were examined at  $-178$  °C using a FEI Tecnai 12 G<sup>2</sup> TWIN transmission electron microscope equipped with a Gatan 626 cold stage, and the images were recorded (Gatan model 794 CCD camera) at 120k V in low-dose mode. Samples for HRTEM imaging were prepared by placing a droplet of the dispersion on a TEM grid (300 mesh Cu, Ted Pella Ltd.) and allowing the solvent to evaporate.

## Results

DSC was used to characterize the thermal aggregation of Pluronic block copolymers in dispersions of carbon nanotubes. DSC allows the evaluation of thermodynamic properties (heat capacity, enthalpy, and transition temperatures) over the scanned temperature range, thus providing information about the macroscopic phase behavior of the system.<sup>37</sup> Molecular characteristics of the SWNT-Pluronic system were obtained using spin-probe EPR. EPR maps the microenvironment of the spin probe, providing information about the dynamics (viscosity) and polarity of its environment.

**DSC of CNT-Pluronic Dispersions.** Dispersions of MWNT and individual SWNT were prepared following the previously published procedure.<sup>24,26,38</sup> In Figure 2, we present macroscopic (Figure 2b) and microscopic (Figure 2c,d) images of SWNT dispersions and MWNT (Figure 2e) using different Pluronic block copolymers as dispersing agents.

As was previously reported by us, the formed dispersions are stable and long-lived.<sup>25</sup> Cryo-TEM suggests<sup>24,38</sup> that the most abundant species in similar dispersions are individual tubes and small bundles, in agreement with neutron scattering results of similar systems.<sup>39</sup>

DSC measurements of aqueous solutions of different Pluronics at a few concentrations were carried out. The main observation

(28) Paterson, I.; Armstrong, J.; Chowdhry, B.; Leharne, S. *Langmuir* **1997**, *13*, 2219–2226.

(29) Supporting evidence for this view is found in DSC studies of PPO aggregation where a similar peak is observed. Chowdhry, B. Z.; Snowden, M. J.; Leharne, S. A. *Eur. Polym. J.* **1999**, *35*, 273–278.

(30) Schneider, D. J.; Freed, J. H. In *Biological Magnetic Resonance. Spin Labeling*; Berliner, L. J., Reuben, J., Eds.; Plenum: New York, 1989; Vol. 8, Chapter 1.

(31) Morriset, J. D. *Spin Labeling, Theory and Applications*; Berliner, L. J., Ed.; AP: New York, 1976; Chapter 8.

(32) Caldararu, H. *Spectrochim. Acta A* **1998**, *54*, 2309–2336.

(33) Carageorghopol, A.; Caldararu, H. *Electron Paramagnetic Resonance*; The Royal Society of Chemistry: Letchworth, U.K., 2000; Vol. 17, p 205.

(34) Ruthstein, S.; Frydman, V.; Kababya, S.; Landau, M.; Goldfarb, D. J. *Phys. Chem. B* **2003**, *107*, 1739–1748.

(35) Ruthstein, S.; Frydman, V.; Goldfarb, D. J. *Phys. Chem. B* **2004**, *108*, 9016–9022.

(36) Carageorghopol, A.; Caldararu, H.; Dragutan, I.; Joela, H.; Brown, W. *Langmuir* **1997**, *13*, 6912–6921.

(37) Garti, N., Ed. *Thermal Behavior of Dispersed Systems*; Surfactant Science Series 93; Marcel Dekker, Inc.: New York, Basel, 2001.

(38) Shvartzman-Cohen, R.; Levi-Kalishman, Y.; Nativ-Roth, E.; Yerushalmi-Rozen, R. *Langmuir* **2004**, *20*, 6085.

(39) Dror, Y.; Pyckhout-Hintzen, W.; Cohen, Y. *Macromolecules* **2005**, *38*, 7828–7836.

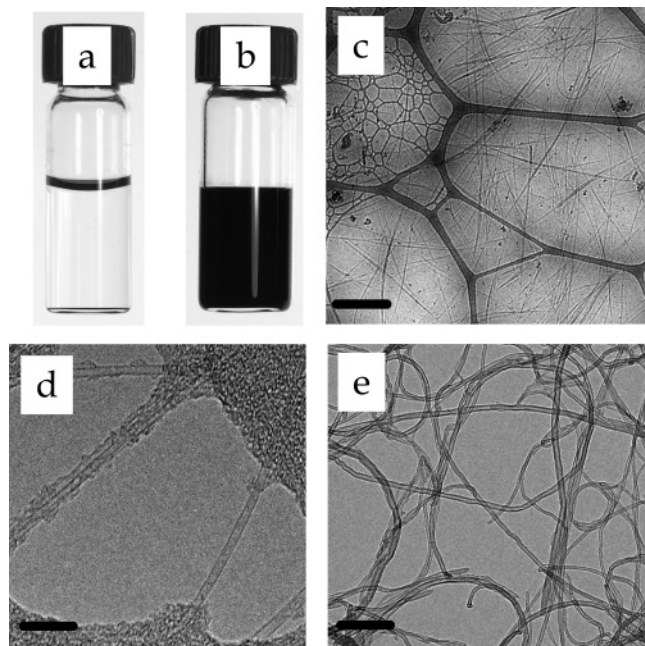


**Figure 2.** Vials containing (a) aqueous solution of F127 (4 wt %) and (b) aqueous dispersion of 0.5 wt % SWNT(AP) in 1 wt % P123. TEM images of aqueous dispersions of CNT: cryo-TEM image of (c) an aqueous dispersion of 0.5% SWNT in F108 1 wt % (scale bar = 500 nm) and HRTEM images of (d) 1 wt % SWNT(AP) in PE10500 (scale bar = 10 nm) and (e) 0.1 wt % MWNT in 1 wt % P84 (scale bar = 200 nm).

in DSC studies of Pluronic solutions is a large endothermic peak (Figure 1), commonly assumed to mark the SA of Pluronics into micelles. The peak results from the dehydration of the PPO groups.<sup>29,40</sup> The peak shape is asymmetric due to a negative heat capacity change at the transition ( $\Delta C_p < 0$ ) which is indicative of an aggregation process, and the normalized enthalpy per PPO group is of the order of 20 cal/g of PPO.

In Figure 3, we present DSC thermograms of carbon nanotube dispersions of two different Pluronic block copolymers. As can be seen, the presence of SWNT and MWNT significantly affects the thermal transition. In particular, while the traces of the native Pluronic solutions (dashed lines) show the typical broad peaks (extending over more than 10 K), those of the dispersions (solid lines) are significantly modified.

Two classes of modifications are observed: In the class represented by Figure 3a, the presence of SWNT or MWNT shifts the thermal transition to a higher temperature as compared to the native solution, the transition enthalpy is reduced, and the peak half-width is narrowed. A second type of behavior is presented in Figure 3b where, in addition to the above-mentioned modifications, a new feature appears in the thermogram, a pre-micellization step (solid line). A systematic DSC study of different Pluronics at different concentrations was carried out, and the data are presented in Table 2. We found that in all the measured dispersions the presence of the nanotubes resulted in a reduction of the transition enthalpy and an upshift of the transition temperature, as compared to the native solutions. The observed reduction of peak enthalpy was found to scale with the relative nanotube concentration, with up to a 50% reduction of the molar enthalpy in a dispersion of 0.5 wt % SWNT in 1 wt % F127. As to the effect of SWNT on the CMT, an upshift of 10 K was measured in a SWNT dispersion of 0.5 wt % F108.

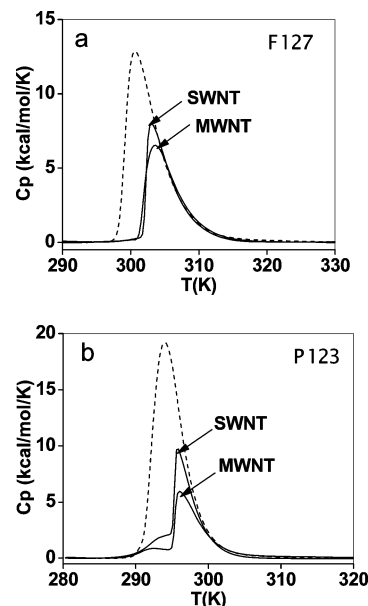


**Figure 3.** Baseline subtracted DSC thermograms of Pluronic–CNT dispersions (solid line) compared to the corresponding native Pluronic solutions (dashed line). The concentration of the relevant Pluronics is 1 wt %, and the dispersions contain 0.5 wt % CNT: (a) F127 1 wt % and (b) P123 1 wt %.

**Table 2. Summary of the CMT and  $\Delta H$  Obtained via DSC Experiments**

polymer	polymer concn (wt %)	additive (0.5 wt %)	CMT (K)	$\Delta H$ (kcal/mol)
F127	1%	none	299.3	80.7
		MWNT	301.8	39.7
	4%	SWNT	302.3	38.4
		none	296.1	83.8
		MWNT	297.0	62.4
		SWNT	296.8	67.0
10%	none	292.4	83.4	
	MWNT	293.7	58.7	
	SWNT	292.7	78.0	
P123	1%	none	292.1	104.1
		MWNT	295.5	31.6
		SWNT	295.4	40.4
P103	1%	none	294.6	83.5
		MWNT	297.6	38.5
F108	0.5	none	307.5	47.8
		MWNT	314.7	13.9
	1	SWNT	317.1	9.7
		none	305.9	58.8
F88	4	MWNT	311.1	22.1
		SWNT	309.1	33.7
		none	309.5	41.5
P84	5	MWNT	311.4	32.4
		SWNT	311.2	36.8
		none	298.6	52.0
		MWNT	299.4	46.1
		SWNT	299.5	45.2

MWNT showed a similar trend. Interestingly, the tailing part of the peak remained unaffected.

We observed that all the experiments reported in Table 2 belong to one of the two classes of thermograms reported in Figure 3. Analysis of the results suggests that the type of the observed thermogram is correlated with the PEO content of the Pluronics: a pre-micellization transition (as presented in Figure 3b) appears only for a relatively short PEO moiety. P123 (with two PEO blocks each of 20 EO units), P103 ( $2 \times 16$  EO units), and P104 ( $2 \times 25$  EO units) exhibit a pretransition. For Pluronics with a

(40) Zana R., Ed. *Surfactant Solutions, New Methods of Investigation*; Marcel Dekker, Inc.: New York, Basel, 1987.

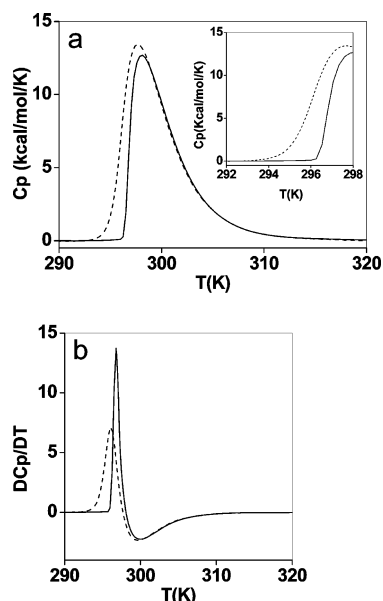


**Figure 4.** Aqueous solution of 4 wt % F127 (dashed line) and a dispersion containing 1 wt % SWNT (solid line) in 4 wt % F127. (a) Normalized DSC output and (inset) a higher magnification of the trace at the peak onset and (b) the derivative of (a).

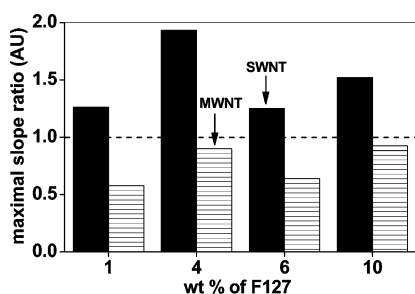


**Figure 5.** Calculated values of the maximal slope of the DSC trace. Different concentrations of F127 containing 0.5 wt % SWNT and MWNT were measured. The values were normalized to native solutions at the same concentrations (dashed line).

long PEO block as in F108 ( $2 \times 130$  EO units), F88 ( $2 \times 100$  EO units), and F127 ( $2 \times 106$  EO units), the thermograms measured in the dispersions resemble that presented in Figure 3a.

Below, we analyze separately the two types of behaviors, using F127 for the investigation of systems that do not show a pretransition step and P103 for the second class. In Figure 4, we present an analysis of the initial slope of the endothermic peak marking the CMT in thermograms of a solution of F127 (dashed line) as compared to a dispersion of SWNT (solid line).

Analysis of the slope of the DSC peak indicates that in the presence of SWNT the peak slope is steeper at the onset of the transition, as compared to the trace measured for the native solution. We find that this phenomenon is generic, and dispersions of SWNT in different Pluronics and at a variety of concentrations systematically exhibit steeper initial slopes as compared to the native Pluronic solutions of similar concentration. The effect of MWNT is different, and the initial slope is more moderate than that of the native solution, as indicated in Figure 5. It is well accepted<sup>27,40</sup> that an increase in the slope of the peak is indicative of the formation of larger aggregates, sometimes referred to as a “higher cooperativity”, where an initial slope that is perpendicular to the baseline would indicate a first-order phase transition (as the aggregation number tend to infinity). We relate to this point in the Discussion section.

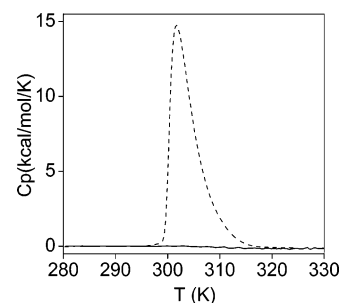
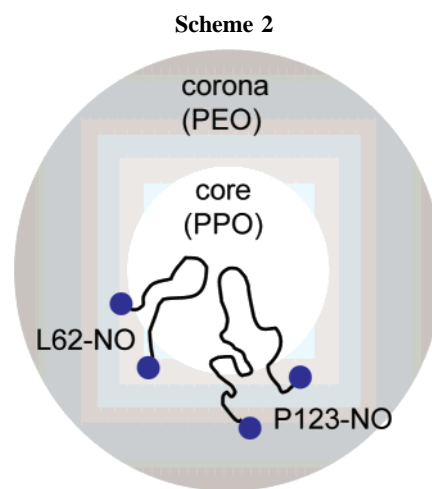


**Figure 6.** Normalized DSC thermogram of F127 0.5 wt % containing 0.5 wt % CB (solid line) compared to a native solution of F127 0.5 wt % (dashed line).



A different behavior was observed in dispersions of P123, P104, and P103 (Figure 3b and the Supporting Information). The thermograms of these dispersions are characterized by the appearance of a pretransition feature (a “step”) of a moderate slope, and a small enthalpy change. The very small enthalpy change may indicate that the process does not involve desolvation of PPO moieties and may suggest some type of surface aggregation among the adsorbed, desolvated moieties preceding the CMT.

An additional experiment was carried out using dispersions of carbon black (CB). CB is composed of carbonaceous particles of similar composition and surface area as CNT. Yet, while CB is a typical colloidal particle of mesoscopic dimensions and spherical geometry, both SWNT and MWNT are cylindrical structures of nanometric tube diameter. DSC data of Pluronic dispersions of CB are presented in Figure 6.

The DSC thermograms reveal that, in CB dispersions of low polymer concentration where most of the chains are adsorbed, thermal transition is not detected, suggesting that chains adsorbed onto CB do not exhibit a CMT.

**EPR of Pluronic F127 Dispersions of SWNT.** EPR was used to probe the effect of SWNT on the aggregation of Pluronic F127 in SWNT dispersions as a function of temperature, as described in detail in ref 25. Here, we concentrate mainly on the effect of the SWNT on the CMT as detected by EPR. EPR measurements of solutions of F127 (containing minute amounts of P123-NO and L62-NO) were carried out as a function of temperature for several concentrations of F127. The two spin labeled Pluronics differ in the lengths of the PEO and PPO blocks. Consequently, their nitroxide groups are located within the F127 Pluronic micelles at different locations as presented schematically in Scheme 2.<sup>33</sup> Following ref 33, L62-NO is located close the core/corona interface, whereas P123-NO reports on the central

**Table 3. Transition Temperatures Measured in Aqueous Solutions of F127 via EPR Using Two Different Spin Probes and DSC (Onset Temperature)**

F127 wt %	P123-NO $T_{50/50}^a$ ( $\pm 1$ K)	L62-NO $T_{50/50}$ ( $\pm 1$ K)	DSC $T_{onset}$ ( $\pm 1$ K)
1	300.2	302.4	299
2.5	300.4	302.4	297
4	297.9	303.3	296
1 wt % F127 + 1 wt % SWNT	305.7	307.1	302
4 wt % F127 + 1 wt % SWNT	303.2	304.6	297

<sup>a</sup> Temperature at which  $S_i/S_m = 1$

region of the corona. In each of the cases, the average location of the probe is inferred from the  $a_{iso}$  values (14.9 and 15.2 (at 340 K)) of L62-NO and P123-NO, respectively. In native Pluronic solutions, the EPR spectrum below the CMT corresponds to single species, attributed to individual chains and referred to as  $S_i$ . Above the CMT, the spectrum changes,  $a_{iso}$  decreases, and the correlation time  $\tau_c$  increases, as expected for a Pluronic molecule within a micelle. We refer to this species as  $S_m$ . During the transition from individual chains to micelles, both species coexist and the spectrum is a superposition of the two. The relative contribution of each species to the spectrum was determined by reconstructing the spectrum as a superposition of the spectra of  $S_i$  just below the CMT and  $S_m$  above the CMT. The CMT was taken as the temperature where the relative contributions of the two are equal, and the results are summarized in Table 3. Interestingly, L62-NO, which is situated closer to the core/corona interface, reports consistently a higher CMT than the P123-NO situated in the corona. The presence of the SWNT has two significant effects: (i) While aggregation of the Pluronics (which leads to the reduction of polarity and a lower rotational mobility) still takes place in the presence of SWNT, the transition is significantly shifted to higher temperatures. P123-NO reports a transition at about 5 K higher than in the native solutions, and for L62-NO an upshift of 2–5 K was observed. (ii) While in the native solution  $S_i$  is not present above the CMT, in the SWNT dispersion a significant fraction of  $S_i$  (10–20%) remains also above the CMT (see ref 25).

Another interesting observation is related to the effect of the different additives on the line shape of adsorbed chains, below the CMT, as probed by the two spin probes. EPR spectra of solutions below the CMT reveal that the spectrum depends on the type of the carbonaceous additive present in the dispersion, as shown in Figure 7. We find that the presence of SWNT does not alter the line shape of the P123-NO spectrum as compared to that of the native solution. Very differently, the spectrum of the CB samples indicates the presence of two components: one similar to that found in native F127 solutions (below the CMT), resulting from populations that exhibit correlation times similar to that of the native solution, and, in addition, a significantly broader line (indicated by an arrow in Figure 7a), characteristic of restricted mobility. The broad line is assigned to chains adsorbed onto CB. The spectra of L62-NO, presented in Figure 7b, show a similar behavior with the exception that the relative intensity of the broad component is higher and the width of the spectrum is wider, indicating a slower motion for the adsorbed chains. This is not surprising because of the higher proximity of the nitroxide spin label to the hydrophobic block, which is the part that interacts with the hydrophobic surface of CB. The spectrum of the adsorbed chains narrows as the temperature increases due to increased mobility on the surface (Figure 7c). The observation of two distinct signals for the adsorbed and free chains indicates that they do not exchange on the EPR time scale ( $\sim 10^{-6}$ – $10^{-7}$  s). We recall that the effect of SWNT on the

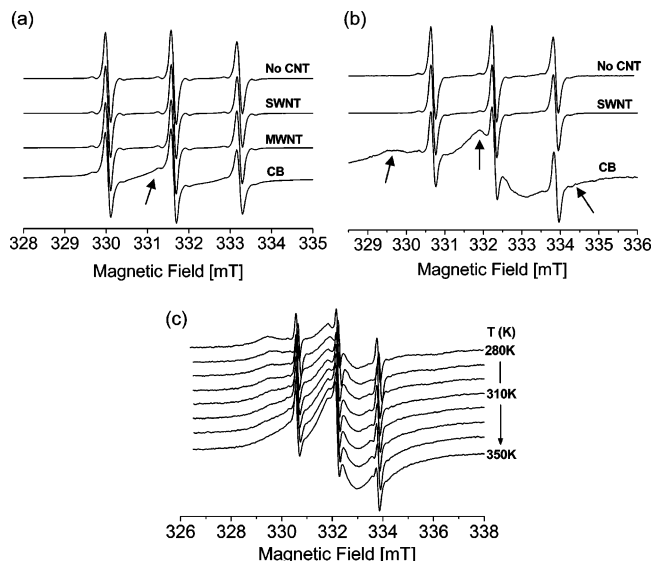


**Figure 7.** EPR spectra of (a) P123-NO in 4 wt % F127 with 1 wt % SWNT, MWNT, or CB, below the CMT (290 K). (b) EPR spectra of L62-NO in 1 wt % F127 with 1 wt % SWNT and CB, below the CMT (290 K). Arrows point to the contribution of the broad component. (c) Temperature dependence of the spectra of L62-NO in a dispersion of 1 wt % CB in 1 wt % F127.

mobility of the polymer chains becomes evident only above the CMT.<sup>25</sup> The difference in the polymer–particle interactions observed in dispersions of CB and CNT is attributed to their different spatial dimensions as compared to the typical dimensions of the polymer chains as discussed below.

## Discussion

In this study, we characterized the temperature induced SA of nonionic block copolymers in the presence of SWNT and MWNT using DSC complemented by spin-probe EPR. The thermal aggregation process of Pluronic block copolymers, marked by the CMT, is complex, and it involves water loss from the PPO moieties (an endothermic transition), a gradual loss of water from the PEO regime, modification of the local composition and decrease of the local polarity, and modification of chain conformations and reduced segmental mobility.<sup>14–16,31–33</sup> The actual sequence of events is not well resolved, and different experimental methods used to investigate the micellization measure different observables. Thus, different techniques often report different values of the CMT.<sup>16,40</sup> In this study, we relate to information obtained from DSC and spin-probe EPR measurements of the very same system on temperature induced SA of Pluronic block copolymers in aqueous solutions. The spin probes used by us report mainly the modification of the dynamics and the local polarity of the PEO regime while the DSC measurements are sensitive to the dehydration of the PPO moieties. Thus, the two techniques provide complementary information revealing the overall behavior of the block copolymers–nanostructures system.

In the main part of the study, we focused on the effect of SWNT on the aggregation of Pluronics as probed by DSC. As was shown before,<sup>24,38,43</sup> Pluronic block copolymers are able to disperse individual nanotubes in aqueous solutions well below

(41) To test a possible effect of the EPR spin probes on the thermal behavior of the solutions and dispersions, we carried out a series of DSC experiments where spin probes (L62-NO and P123-NO) at concentrations of 0.5–1 mM were added to the solutions. The DSC curves were found to reproduce those presented in Table 1, showing that the observed thermal behavior is not affected by the presence of the spin probes.

the CMC and CMT. The stable dispersions are formed via the adsorption of polymer molecules onto CNT and the formation of a steric barrier that prevents aggregation of the nanostructures.<sup>24</sup> In this study, we found that the presence of carbon nanotubes actually modifies the aggregation and SA of the polymers themselves. Both DSC and EPR data (ref 25) suggest that the nanostructures have a profound effect on the temperature and nature of the transition. DSC results (see Table 2) indicate that SWNT and MWNT have three effects on the thermograms: (1) they shift the onset of the transition to higher temperatures; (2) they reduce the overall enthalpy of the transition; and (3) they modify the line shape. The changes in the line shape were found to depend on the type of the tubes and on the Pluronic molecular weight and composition.

We first discuss the effect of SWNT as compared to MWNT. Models that analyze DSC traces of micellization suggest that the reduced peak half-width indicates an increased cooperativity, and a steeper slope is indicative of a large aggregation number where a vertical line characterizes a phase separation.<sup>28,29</sup> In all cases reported here, the DSC peaks in the presence of nanotubes are narrower as compared to those measured in the native solutions. In the case of SWNT, the leading edge is steeper as compared to the peak that characterizes the native solution, while for MWNT the slope showed the opposite behavior. Thus, we may conclude that while both SWNT and MWNT promote cooperativity, SWNT result in the formation of larger aggregates than those formed in native solutions of Pluronics.

Comparison of the transition temperature as measured by the EPR parameters (Table 3) with the CMT measured by DSC indicates that aggregation and the reduced rotational mobility occur in the vicinity of the CMT as measured by DSC.

Below the CMT, there are two populations of polymers: adsorbed molecules and those free in solution. The adsorbed chains are attached via their PPO moieties, while their PEO segments dangle into the solution.<sup>24,26</sup> EPR measurements (Figure 7) suggest that in this regime EPR does not distinguish between chains adsorbed on SWNT and free chains. Practically, the EPR parameters of the spin probes exhibit  $a_{iso}$  values typical of a polar environment and a rotational correlation time  $\tau_c$  of a free chain in solution, suggesting that polymer adsorption onto the SWNT has a minor effect on the microenvironment of the spin label located at the end of the PEO chains (see our ref 25). This is in line with the theoretical argument<sup>7,24</sup> suggesting that polymer adsorption onto a cylinder with nanometer diameter should not perturb the conformations of the PEO moieties. Following previous calculations,<sup>24,25</sup> the PPO–CNT attraction in water is estimated to be of the order of the thermal energy per PPO segment. Thus, in the low-temperature limit, most of the PO segments of the adsorbed chains are in contact with the tubes and are partially dehydrated already below the CMT. This is the origin of the observed reduction in the transition enthalpy in dispersions of Pluronics. The adsorbed PPO moieties do not contribute to the dehydration enthalpy measured by DSC during the thermal transition as much as do the nonadsorbed PEO moieties.

Upon temperature increase, endothermal aggregation is observed. Here, the length of the SWNT becomes relevant: with typical lengths of some micrometers, very long micelle-like aggregates may form, as indeed suggested by comparison of the features of the DSC thermograms to those of the native solutions, the increase in the EPR rotational correlation time  $\tau_c$  of the packed

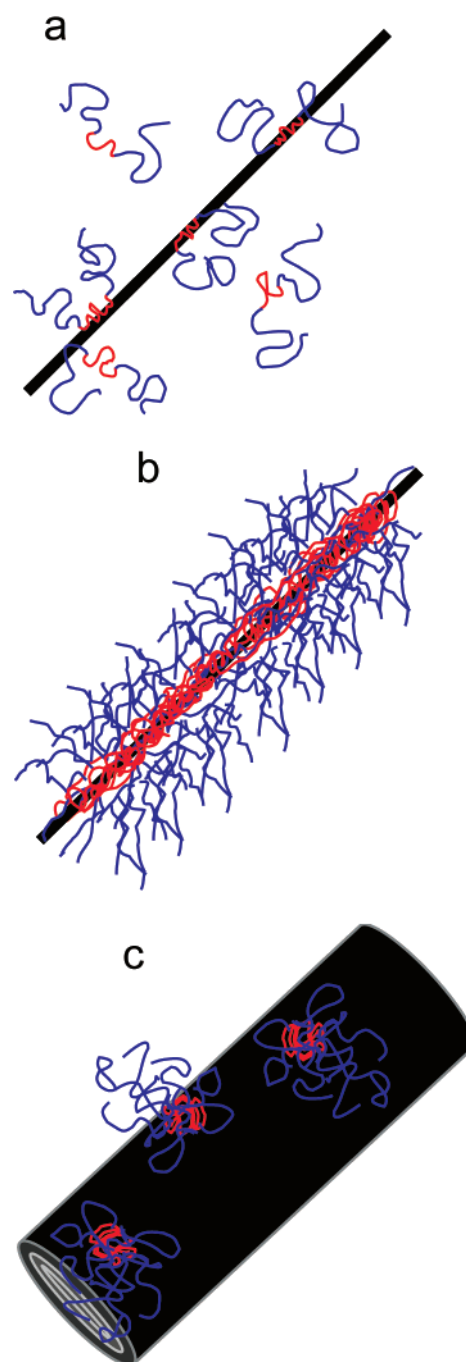


**Figure 8.** Schematics presenting (a) SWNT dispersed by adsorption of Pluronics below the CMT and self-assembly of Pluronics at elevated temperatures for (b) SWNT and (c) MWNT.

chains, and the dependence of the relative amount of  $S_i$  above the CMT and its dependence on the Pluronic/SWNT ratio.<sup>25</sup> Furthermore, we suggest that the aggregates form on the surface of the tubes, whereas the already adsorbed polymers serve as templates for self-assembly, as shown in Figure 8b.

The situation is different for MWNT: here, the tube diameter is of the order of 20 nm, much bigger than the natural dimension of the micellar core. Indeed, DSC slopes suggest the formation of smaller aggregates as compared to SWNT and the native solution (see Figure 8).

One should notice that, while of similar length and aspect ratios of about 1000 and 10 000, MWNT and SWNT are distinguished by a large difference of tube diameter. The value of the tube diameter is significant, as the typical micellar core

(42) Alexandridis, P.; Hatton, T. A. *Colloids Surf., A* **1995**, *96*, 1–46.

(43) Moore, V. C.; Strano, M. S.; Haroz, E. H.; Hauge, R. H.; Smalley, R. E.; Schmidt, J.; Talmon, Y. *Nano Lett.* **2003**, *3*, 1379.

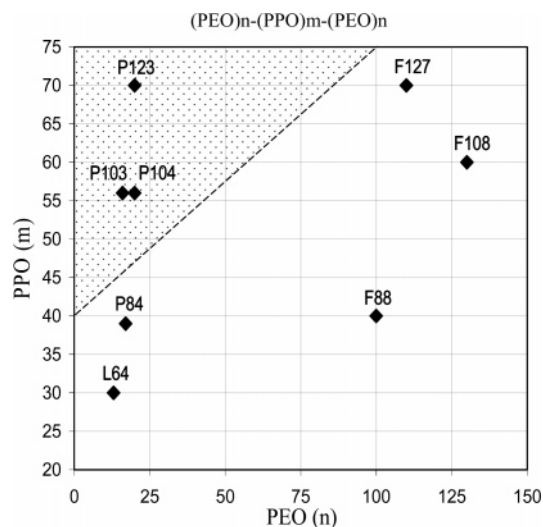


**Figure 9.** Schematic mapping the composition of block copolymers that show a pre-CMT transition in the presence of SWNT (above the line) and block copolymers that do not (below the line).

diameter of native Pluronic micelles is in the range of few nanometers. Thus, while SWNT provide an optimal template for aggregation, MWNT present a huge perturbation to the hydrophobic core of the micelles, suggesting that the smaller aggregates are probably adsorbed on the tubes instead of being an integral part of the core (see Figure 8c).

The size effect is more pronounced in carbon black. CB<sup>44</sup> is a spherical carbonaceous species of similar surface specific area and chemical composition as that of CNT. The typical diameter of individual CB particles is in the range of 30–50 nm, and that of CB aggregates is in the range of some hundreds of nanometers. DSC results indicate that Pluronic chains that adsorb onto CB do not exhibit a thermal transition as the temperature is raised. EPR results further show a significantly different mode of adsorption, where the adsorption restricts considerably the motion of the PEO block, as compared to SWNT, where no restriction was detected. Thus, we observe that adsorption on a colloidal particle is qualitatively different from adsorption onto nanometric particles at all temperatures.

We now relate to the other set of parameters investigated in this study: the composition and chain length of the Pluronic block copolymers.

DSC studies reveal a preaggregation transition in dispersions of SWNT and MWNT that appears when the PEO segments of the dispersing Pluronic are relatively short (Figure 9). The new transition is characterized by a height that is much lower than that of the main peak (low enthalpy). We suggest this transition is related to clustering of adsorbed chains that occurs as the temperature is raised, due to the fact that the solvent becomes a less-good solvent for the PPO segments.<sup>45</sup> Thus, when the PEO chains are short enough, they do not present a significant steric

barrier, and small clusters may form by the adsorption of additional Pluronics on the tubes.<sup>46</sup> When the PEO chains are longer (Figure 9), steric repulsion between adjacent PEO tails prevents small cluster formation. It is only when the temperature is high enough to reduce the solvent quality for the long PEO moieties that a cooperative transition takes place, with the formation of long micelles.

The scenario suggested above is consistent with the experimental observations obtained from DSC and spin-probe EPR. Yet, while the two techniques provide useful data on their local dynamic and thermal behavior, they do not provide structural information, such as the size of the hybrid micelle. Thus, a direct measure of structural features is still required.<sup>47</sup>

## Conclusions

We found that SWNT affect the temperature induced self-assembly of Pluronic block copolymers in aqueous solutions, suggesting the formation of a new type of hybrid SWNT–polymer nanostructures. In SWNT and MWNT dispersions, the dimensions of the tubes were observed to play a crucial role in the interaction. Nanometric 1-D SWNT do not alter the local dynamics of adsorbed chains, and they exhibit high cooperativity at the aggregation stage. MWNT have a minor effect on the local dynamics of adsorbed chains, and they induce the formation of smaller aggregates, as compared to SWNT. Colloidal (mesoscopic, 3-D) particles of similar surface area and chemical composition but of a larger effective radius show a qualitatively different behavior, as adsorbed polymers do not seem to participate in the micellization process.

Thus, the geometry of the nanostructures sets the SA of the polymers and determines the structure of the aggregates. The small diameter of the SWNT (~1 nm) enables the formation of an aggregate that is similar to the native micelle, though much elongated, with the SWNT located at the core of the micelle. For MWNT, the diameter of the tubes is much larger than the native micellar core, and thus, the adsorbed micelles must have a structure different from that of the native aggregates. The size of the CB particles is too large to enable the aggregation process of adsorbed chains.

Understanding of the SA of polymers in the presence of nanostructures is expected to improve our ability to design routes leading to the SA of desired structures.

**Acknowledgment.** R.Y.-R. and D.G. thank the ISRAEL SCIENCE FOUNDATION (Grant No.512/06). R.Y.-R. and I.S. thank the BSF - United States–Israel Binational Science Foundation. R.S.-C. would like to acknowledge the support of the Eshkol scholarship program of the Israel Ministry of Science and Technology. D.G. holds the Erich Klieger chair in Chemical Physics. This research is made possible in part by the historic generosity of the Harold Perlman Family.

**Supporting Information Available:** Raw DSC thermograms of aqueous solutions of F127 and P103 as compared to thermograms of SWNT dispersions at similar concentrations. This material is available free of charge via the Internet at <http://pubs.acs.org>.

LA703782G

(44) Marsh, H., Heintz, E. A., Rodriguez-Reinoso, F., Eds. *Introduction to Carbon Technologies*; Universidad de Alicante: Alicante, Spain, 1997.

(45) For a thorough discussion of the adsorption of block copolymers from a selective solvent, see Marques, C.; Joanny, J. F.; Leibler, L. *Macromolecules* **1988**, *21*, 1051–1059.

(46) It is well-known that in Pluronics adsorbed to hydrophobic surfaces the adsorbed amount increases with increasing temperature as the segregation of both PEO and PPO increases. Tiberg, F. *Langmuir* **1991**, *7*, 2723. Linse, P.; Malmsten, M. *Macromolecules* **1992**, *25*, 5434–5439.

(47) We note here that while cryo-TEM is useful for characterization of the dispersed moieties (SWNT, MWNT, and CB), it cannot be used for characterization of the Pluronic aggregates, as was reported before by Mortensen, K.; Talmon, Y. *Macromolecules* **1995**, *28*, 8829–8834. Pluronic block copolymers as free polymer chains or micelles are practically transparent to the electron beam.